IV MPM Workshop, the University of Utah, March 17-18, 2008

Simulation and Tomography of Closed-cell Polymer Foam in Compression

Hongbing Lu and Nitin P. Daphalapurkar

School of Mechanical and Aerospace Engineering
Oklahoma State University
Stillwater, Oklahoma 74078

Polymer Mechanics Laboratory

Acknowledgements

- Dr. John A. Nairn, for providing the 2D MPM code
- Richard Hornung and Andrew Wissink, LLNL, SAMRAI
- Prof. Jay Hanan, Hrishikesh Bale, Nick Phelps, OSU
- Dr. Francesco De Carlo and Dr. Yong Chu, Advanced Photon Source at Argonne National Laboratories, for providing user time at the Beamline XOR-2-BM-B

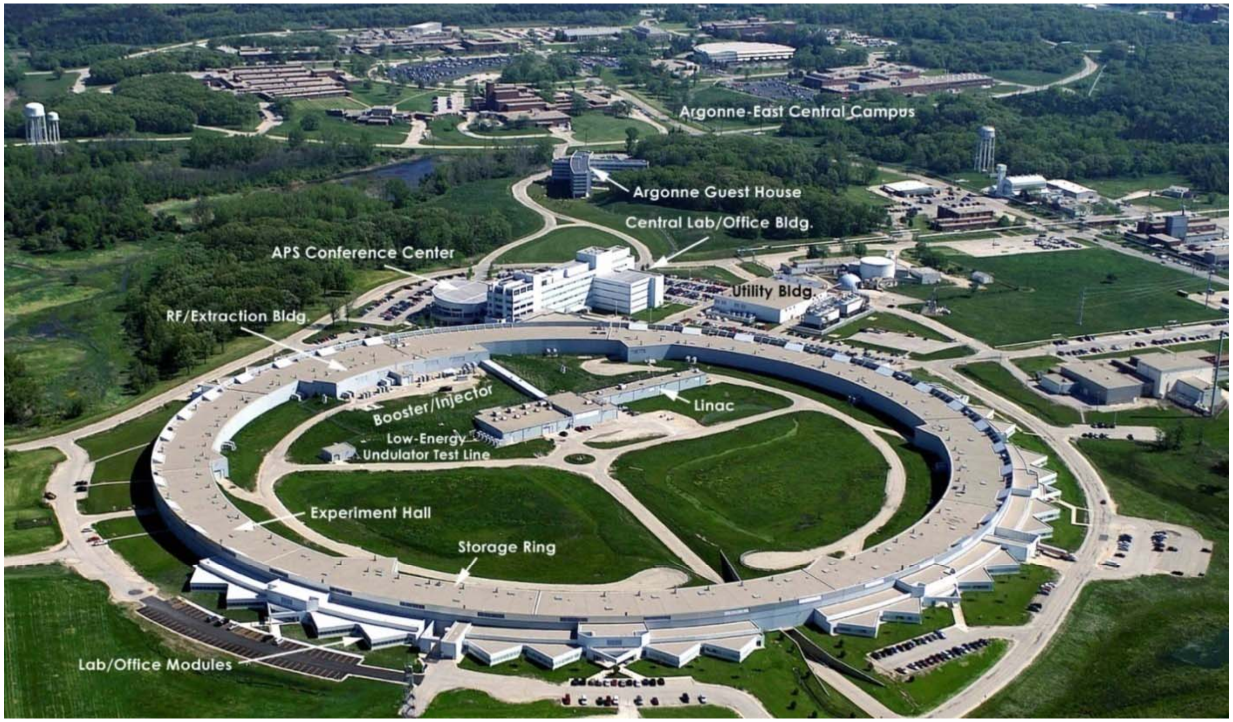

Outline

- In-situ micro-computed tomography (μ-CT) and radiography of Rohacell (Polymethacrylimide, PMI) foam under compression
- Mechanical characterization using compression, and nanoindentation
- Simulation using the Material Point Method (MPM)

Applications for PMI Foam

- Rohacell A foam is primarily used in aircraft as cores for composite sandwich structures up to 266 ºF and 45 psi

- As cores for sandwich structure applications realized by all composite manufacturing processes in aerospace/aircraft marine, sporting goods, wind energy, medical beds, automotive, electronics, energy absorption for crash protection, and others.

- Sandwich structures where electric conductivity is required within the core structure.

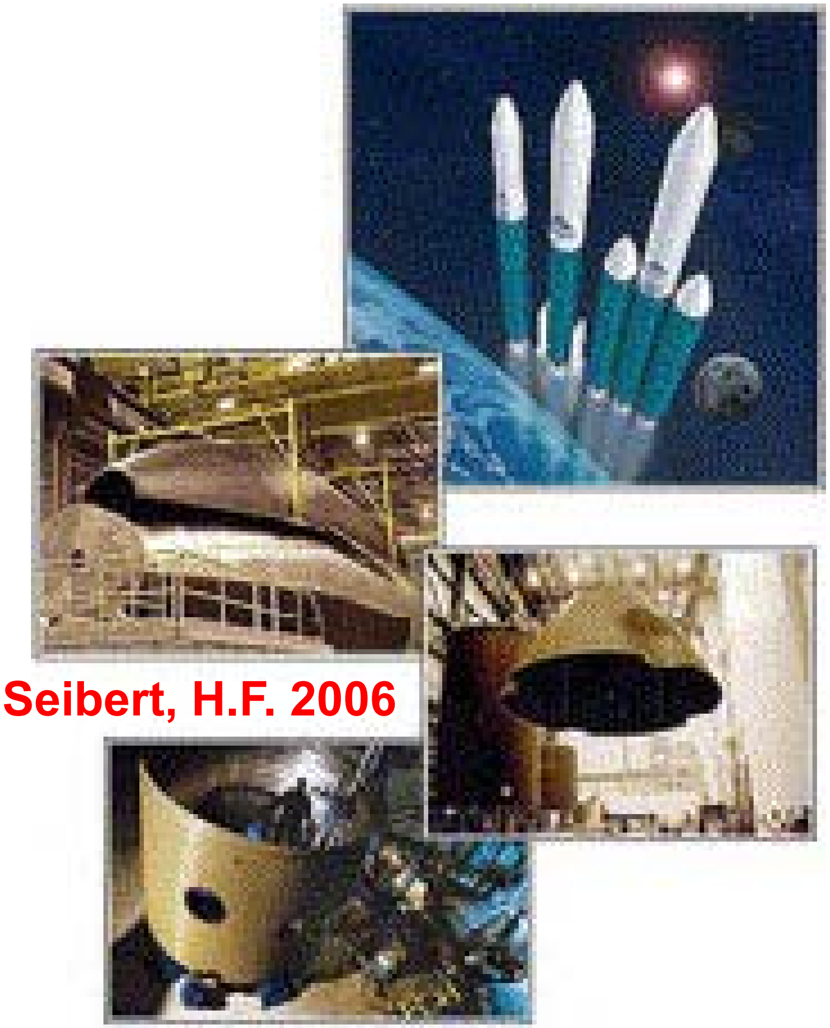

Seibert, H.F. 2006

PMI cored components for Delta 4: payload fairing; payload adapter; interstage; centre body; thermal shield; booster nose cones.

Compressive Stress-Strain Curve of PMI Foam

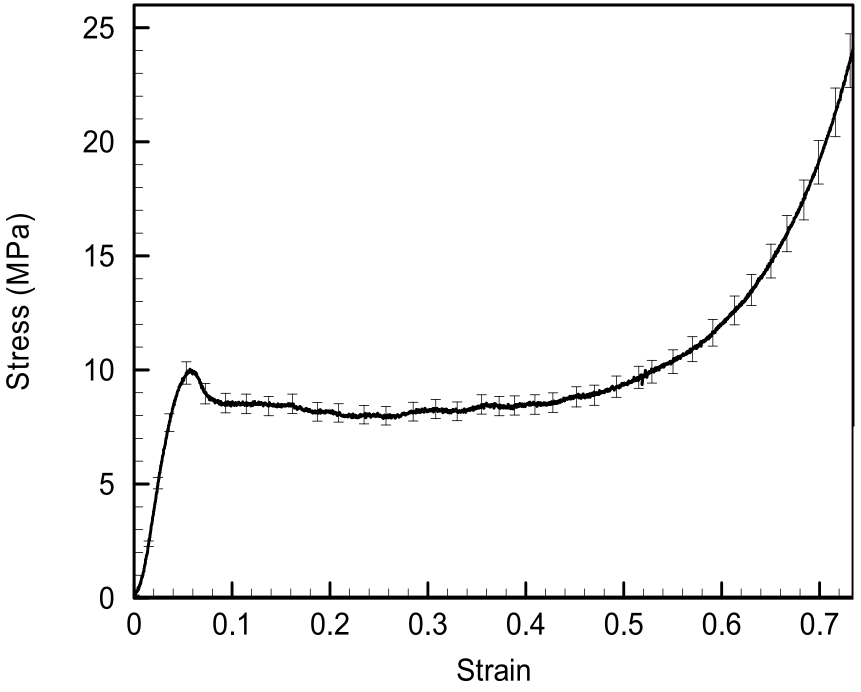

Machine compliance was corrected in compression.

Digital Image Correlation (DIC) was used to measure surface deformations in tension.

Specific energy absorption up to 56% strain: 25.5 J/g, up to 73%: 35.0 J/g.

For a typical high strength dual phase (Martensite/ferrite) steel: 12-15 J/g.

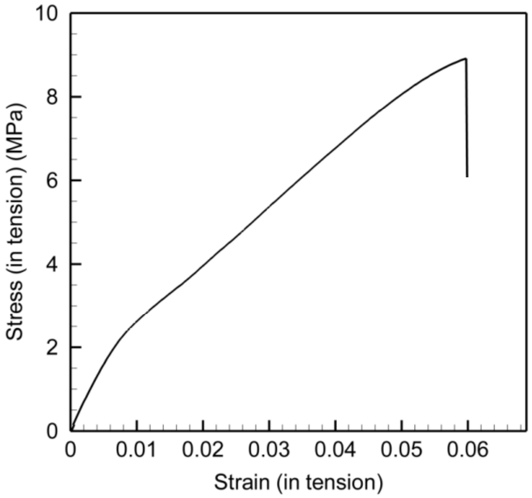

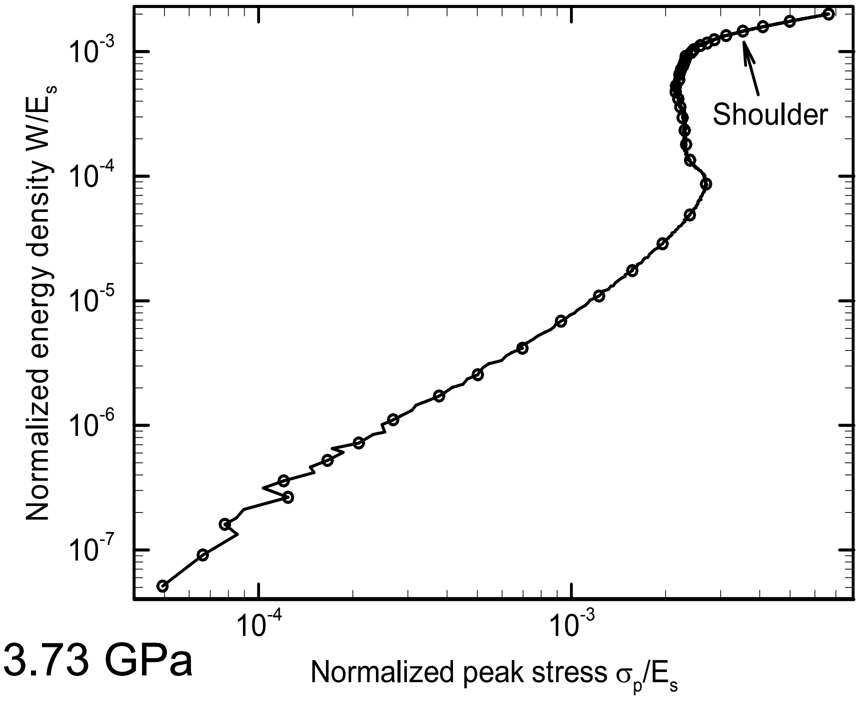

Es = 3.73 GPa

Radiography and Tomography Setup

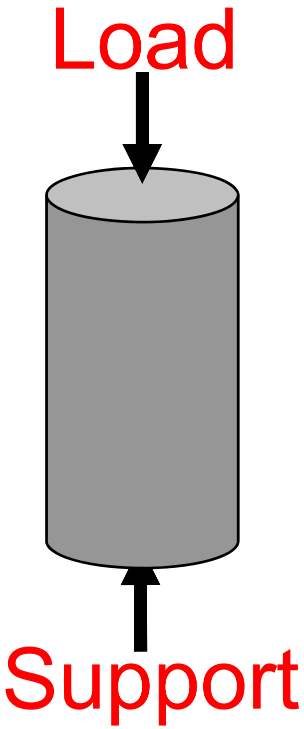

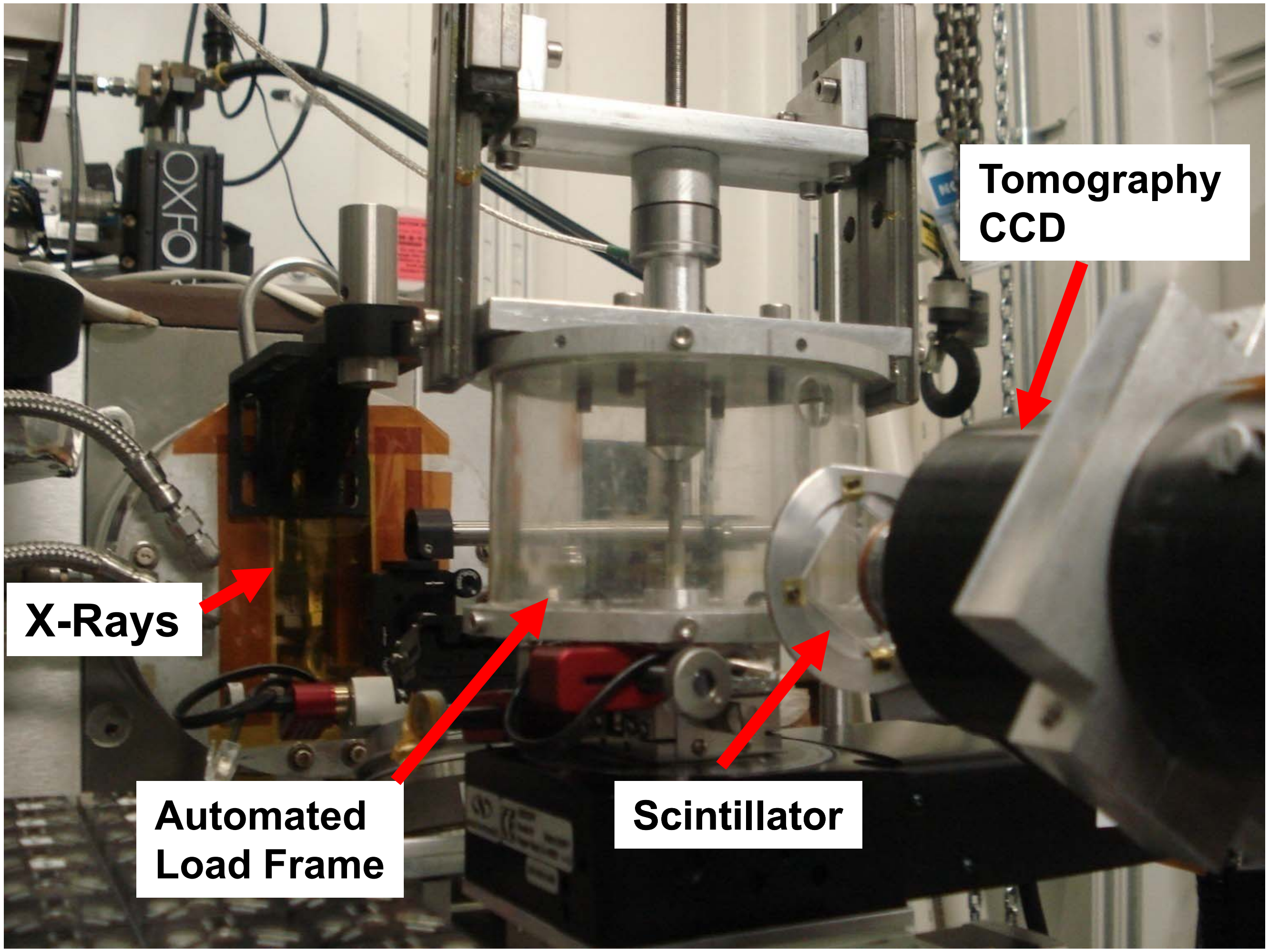

Argonne National Laboratories, 2-BM-B

Micro-Computed Tomography (µ-CT)

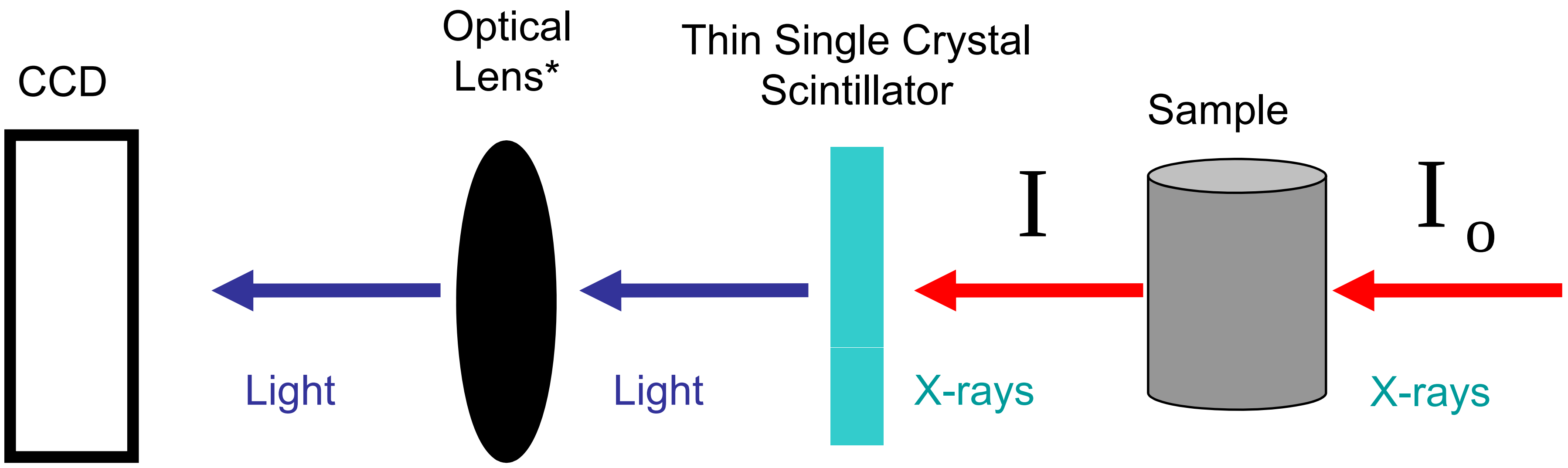

CCD

Optical Lens*

Thin Single Crystal Scintillator

Sample

I

I_o

Light

Light

X-rays

X-rays

* Low depth of field, reject scattered light photons.

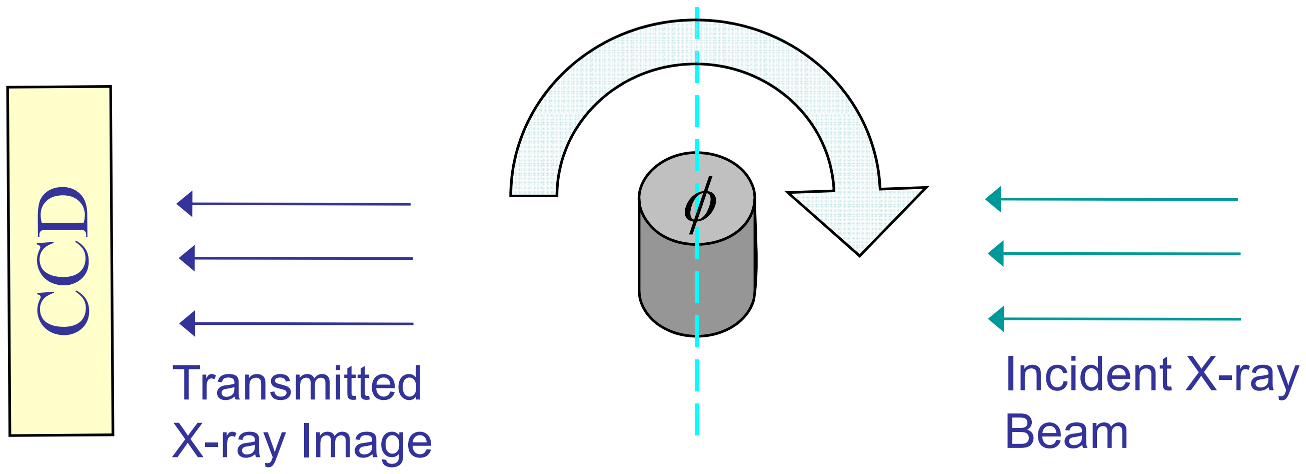

CCD

ϕ

Transmitted X-ray Image

Incident X-ray Beam

Radiographic and Tomographic Images

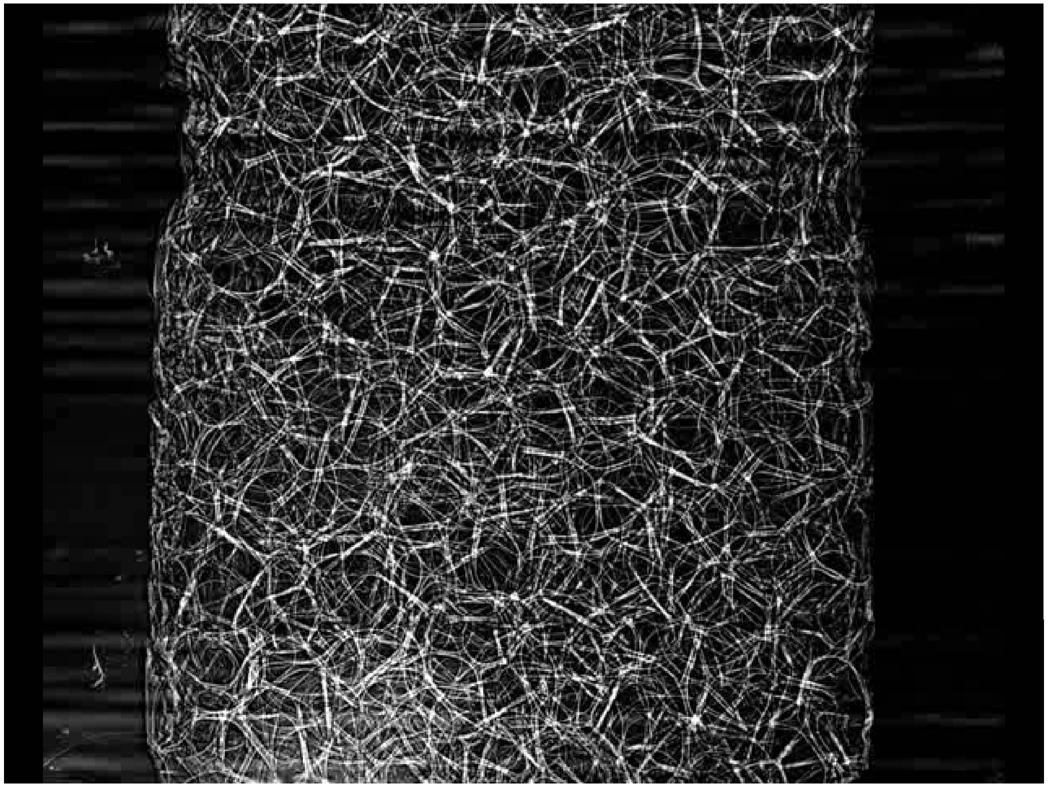

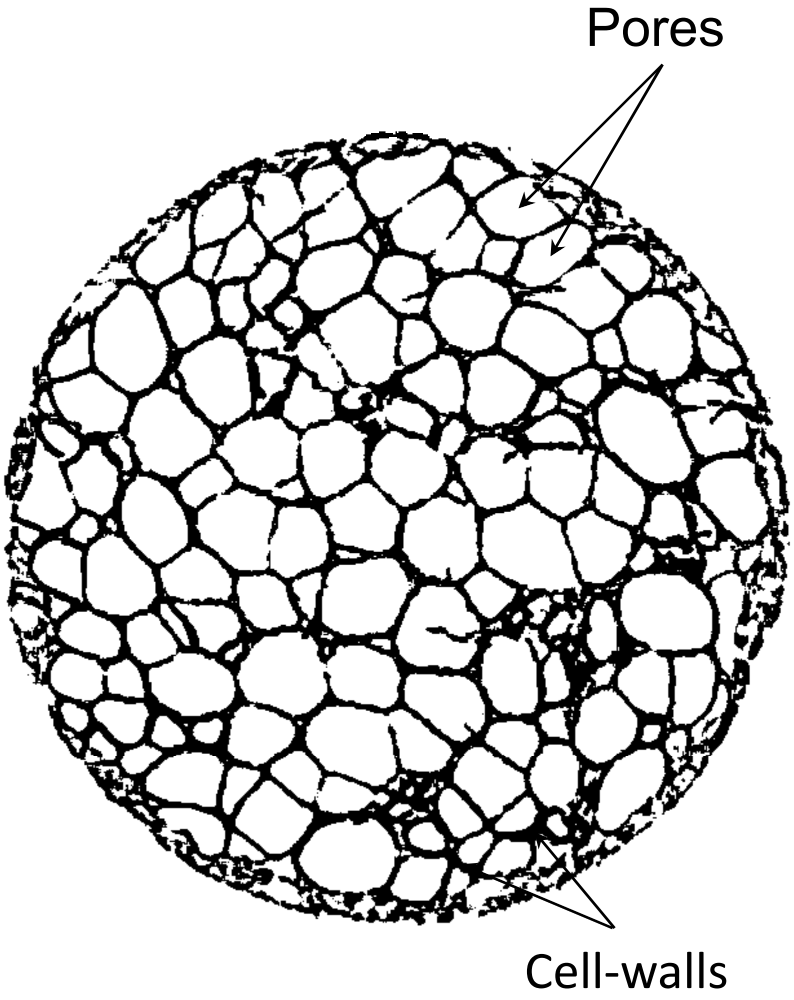

μ-Tomographs at Several Deformed States

1. Initial buckling
2. Cells change shape
3. First collapse
4. Flatening (not total) with residual cells
5. Finished (Highest contact)

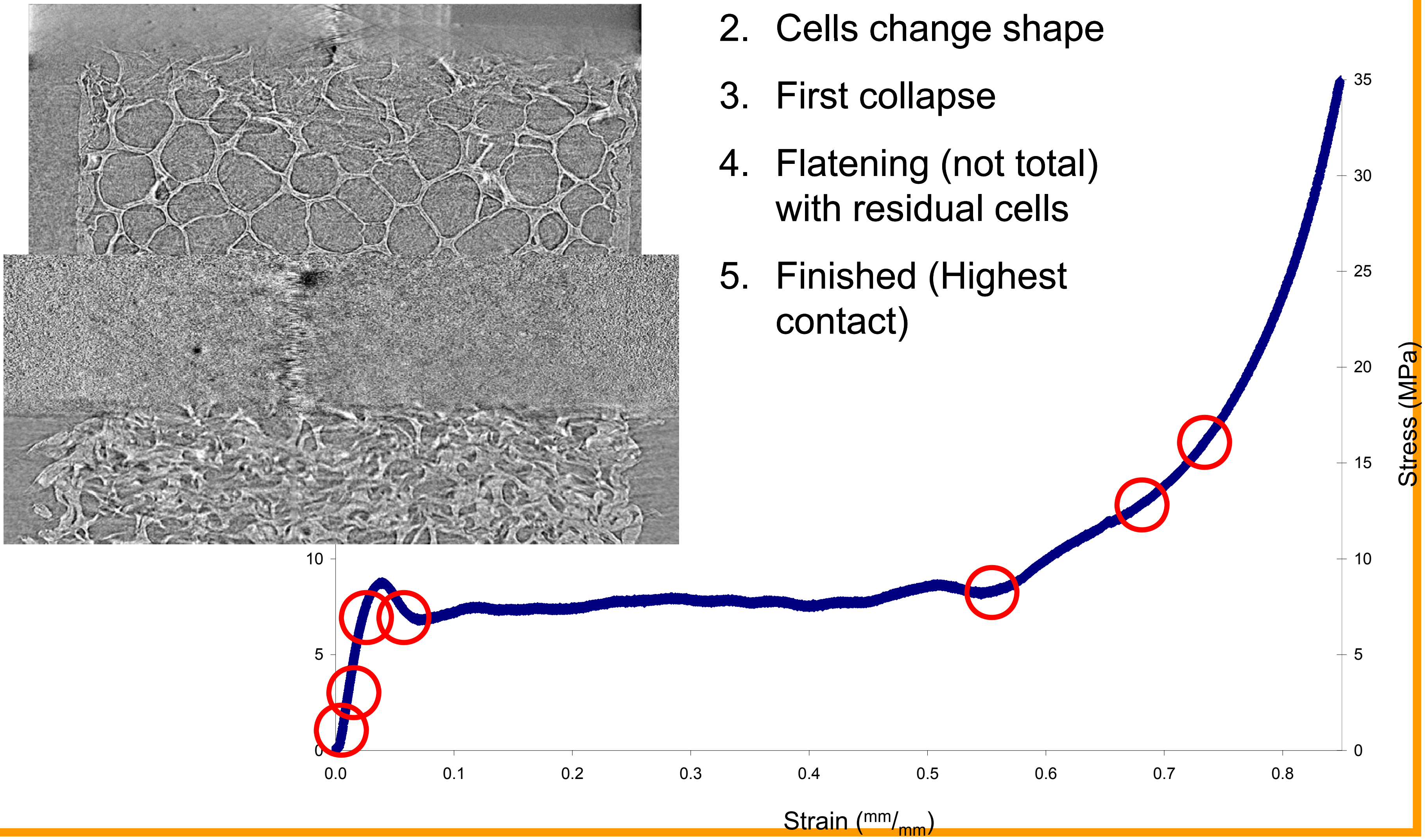

Overview of MPM & GIMP

MPM: Material Point Method
GIMP: Generalized Interpolation Material Point Method

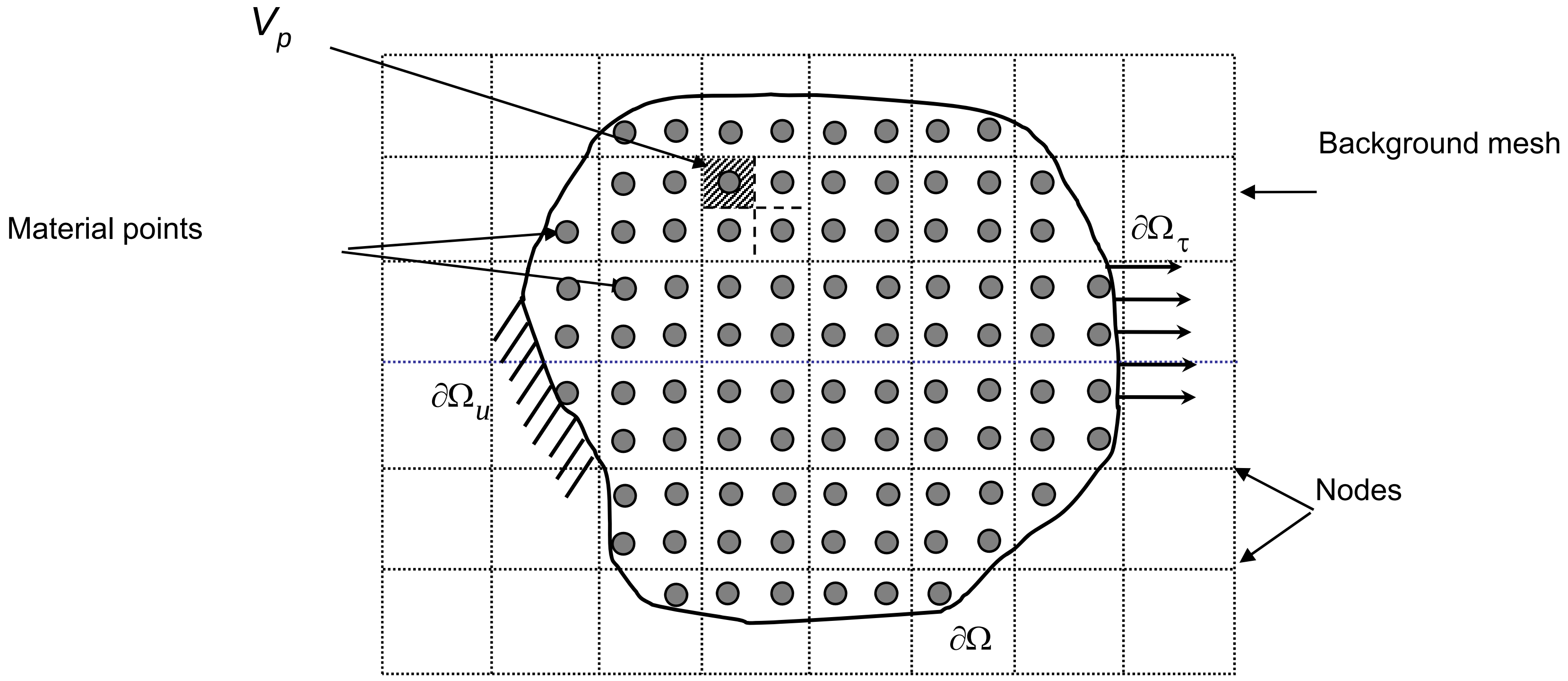

- Harlow, 1964; Brackbill *et al.* 1987; Sulsky *et al.* 1995; Bardenhagen and Kober 2000, 2004; Tan and Nairn 2002; York *et al.* 1999; Banerjee, 2005, Bardenhagen *et al.* 2000; Bardenhagen and Brydon, 2005; Bardenhagen and Brackbill, 1998; Ayton *et al.* 2001; Chen and Brannon, 2002; Nairn, 2004; Hu and Chen, 2003; Guilkey *et al.* 2005; Shen and Chen, 2005, Lu *et al.* 2006; Schreyer *et al.* 2006

GIMP Simulation: Reconstruction and Modeling

- **Discretization: Voxels ➔ Material points**

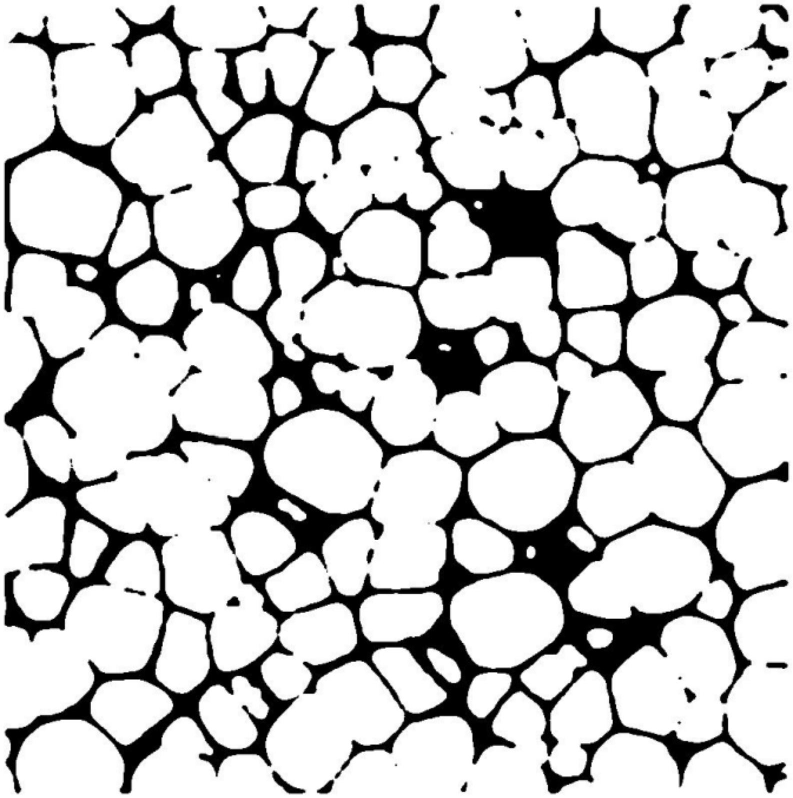

A Section of a Tomographic Image
(Grayscale Image)

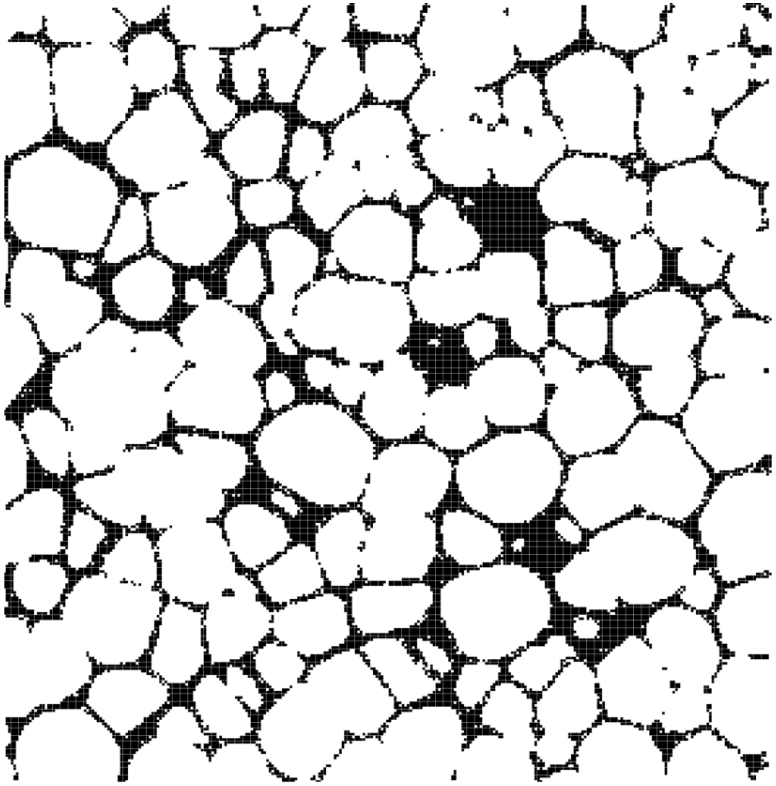

A Section in the MPM Model
(binary)

GIMP Discretized Model

Porosity: 70.6%
Avg. Cell size: 0.32 mm
Avg. Wall thickness: 0.05 mm
Resolution: 8 µm / voxel

Tomographic image acquired using Scanco µCT-40 at OSU.

Tomographic Image

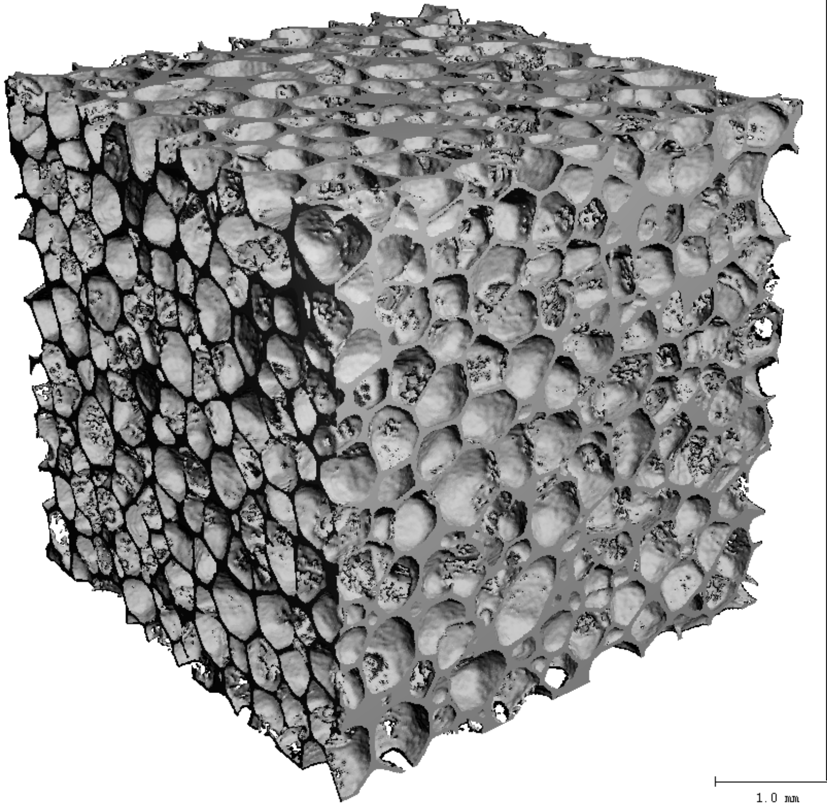

MPM Model

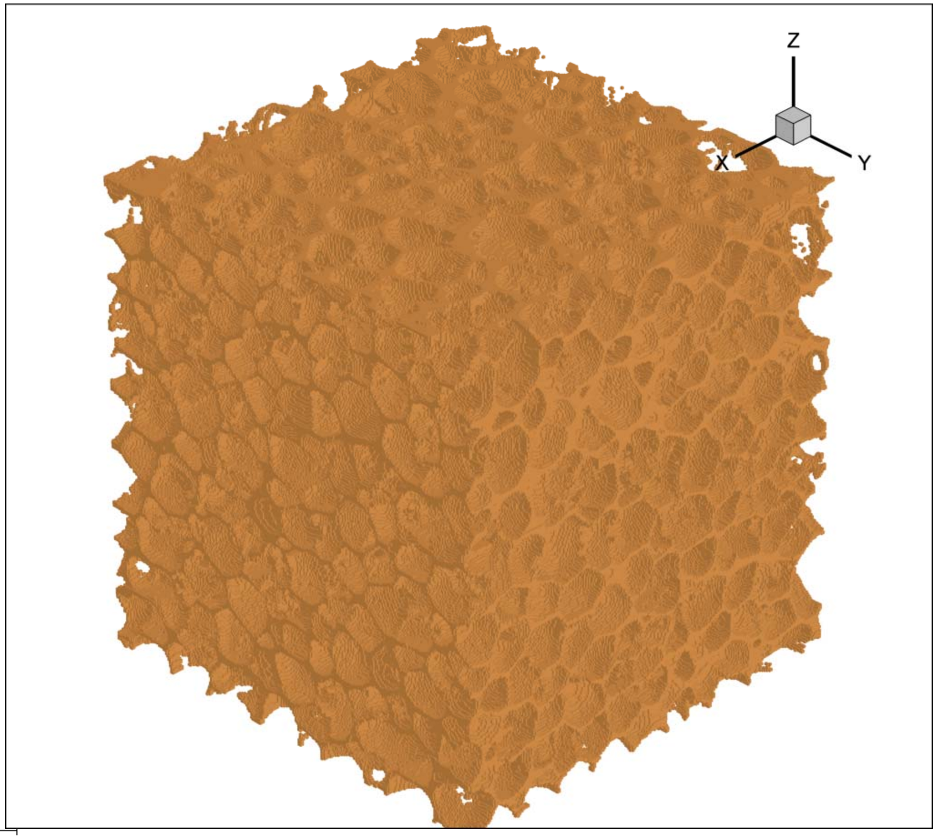

Nanoindentation on the Cell-walls

Direct Measurement of the Mechanical Properties of Cell-walls

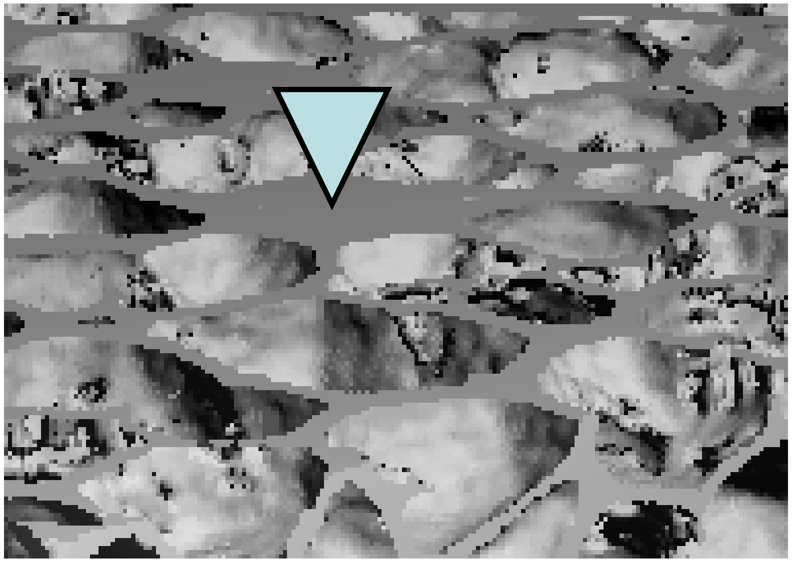

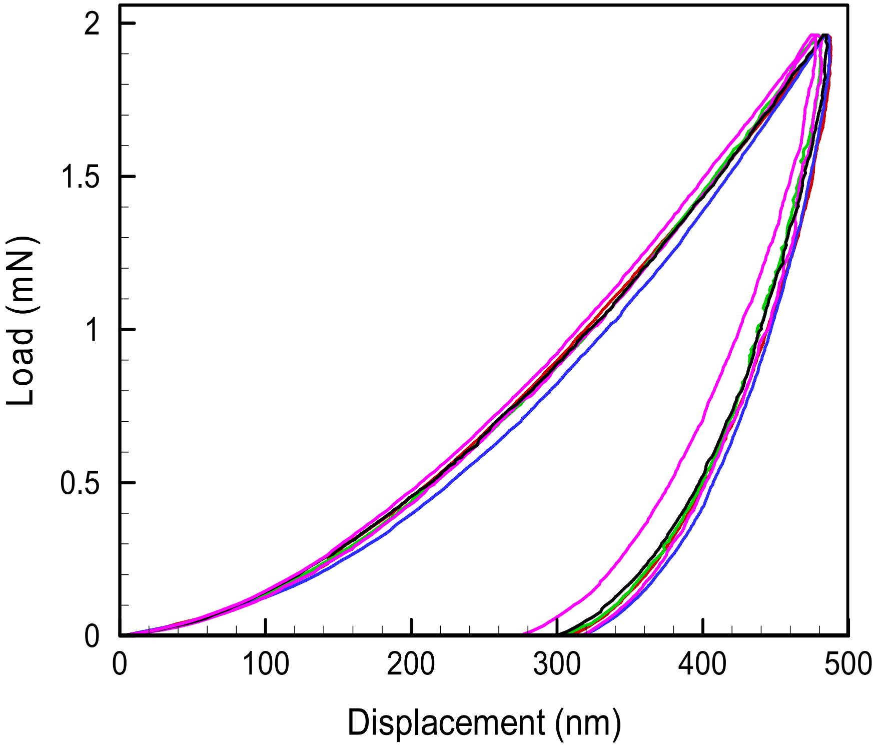

Small pieces of PMI foam were embedded in epoxy. The surface was polished using a minimum abrasive size of 50 nm (Buehler). The sample was annealed to relieve the stresses. A diamond Berkovich indenter tip was used. A constant-rate loading history was used in all nanoindentation tests.

Nanoindentation

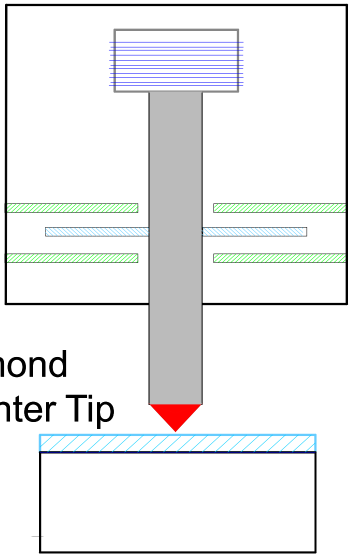

Force Generator

Displacement Gauge

Diamond Indenter Tip

Sample

Substrate

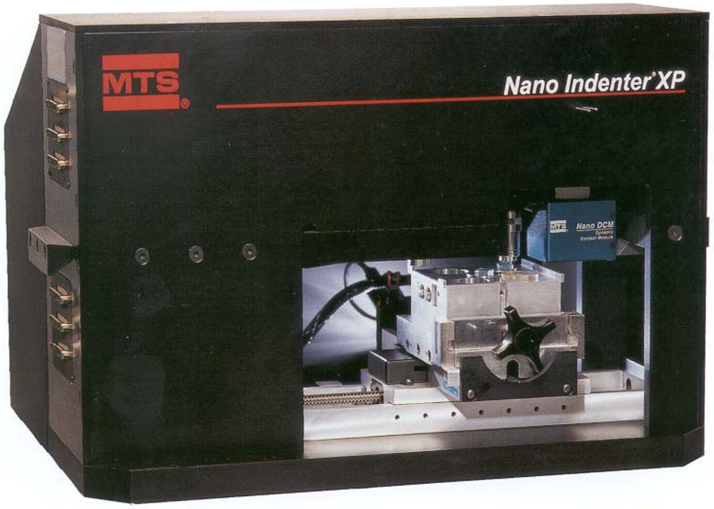

MTS Nano Indenter XP

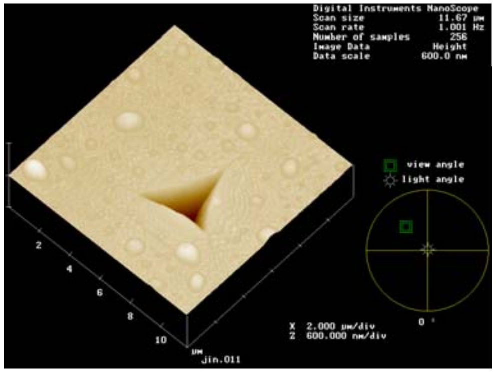

An indent on silicon

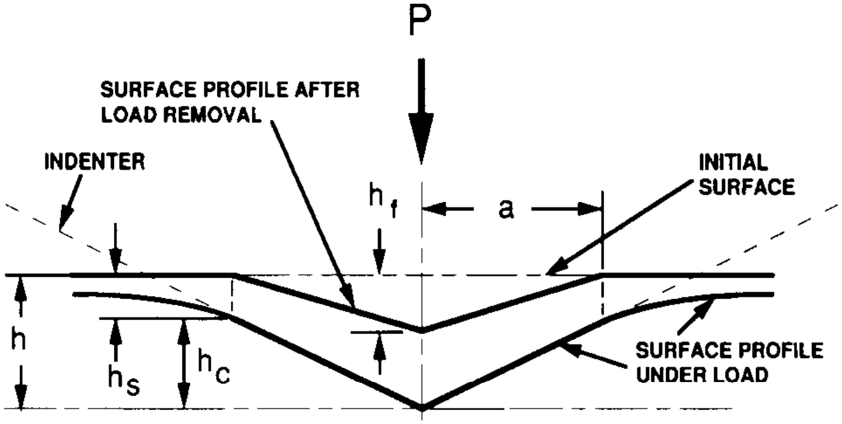

Schematic of indentation profile

(Oliver and Pharr, 1992)

The Oliver-Pharr Approach (1992)

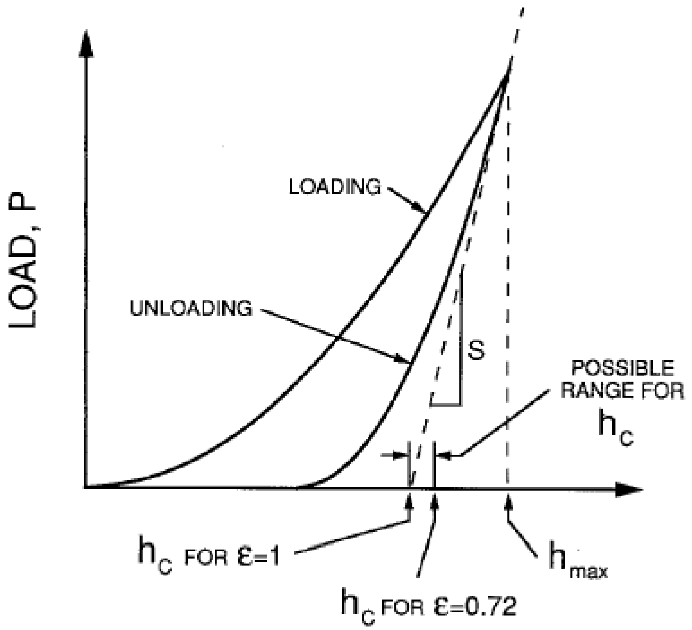

A typical nanoindentation P-h curve

Using this approach, the Young's modulus of PMI cell wall was determined as 9.6 GPa, much higher than the actual value, in the neighborhood of 4 GPa.

$$P = C(h - h_f)^m$$

[From Sneddon's solution (1965)]

$$S = \frac{dP}{dh} = \frac{2}{\sqrt{\pi}}\sqrt{A}E_r$$

$$\frac{1}{E_r} = \frac{1-\nu^2}{E} + \frac{1-\nu_i^{\;2}}{E_i}$$

$$A = a_0 h_c^{\;2} + a_1 h_c + a_2 h_c^{\;1/2} + a_3 h_c^{\;1/4} + a_4 h_c^{\;1/8} \,..$$

(Indenter tip calibration)

$$h_c = h - h_s = h - \varepsilon\frac{P}{S}$$

A Viscoelastic Method to Determine the Viscoelastic Properties by Nanoindentation

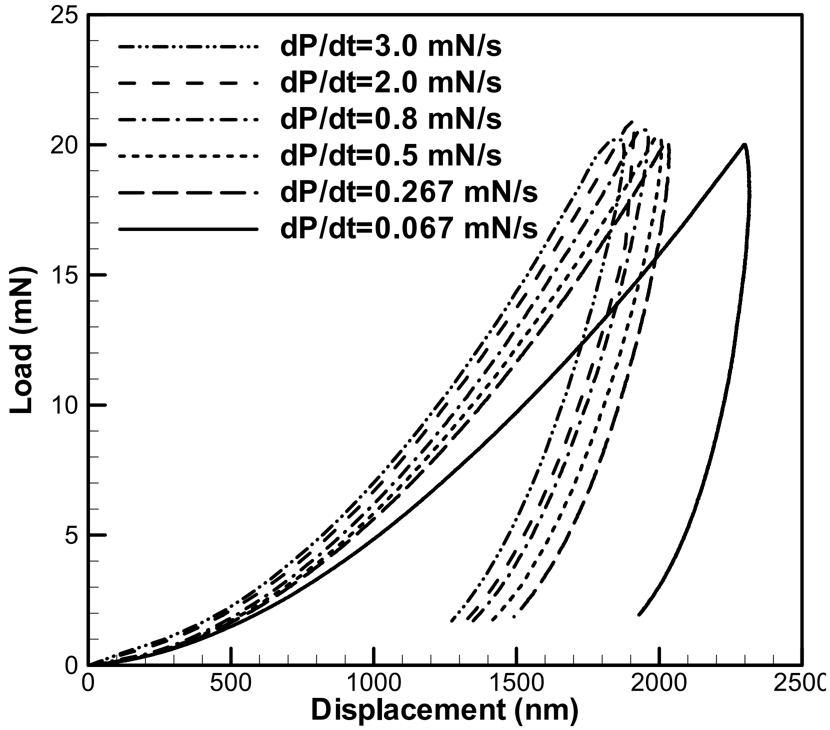

PMMA, using Berkovich indenter

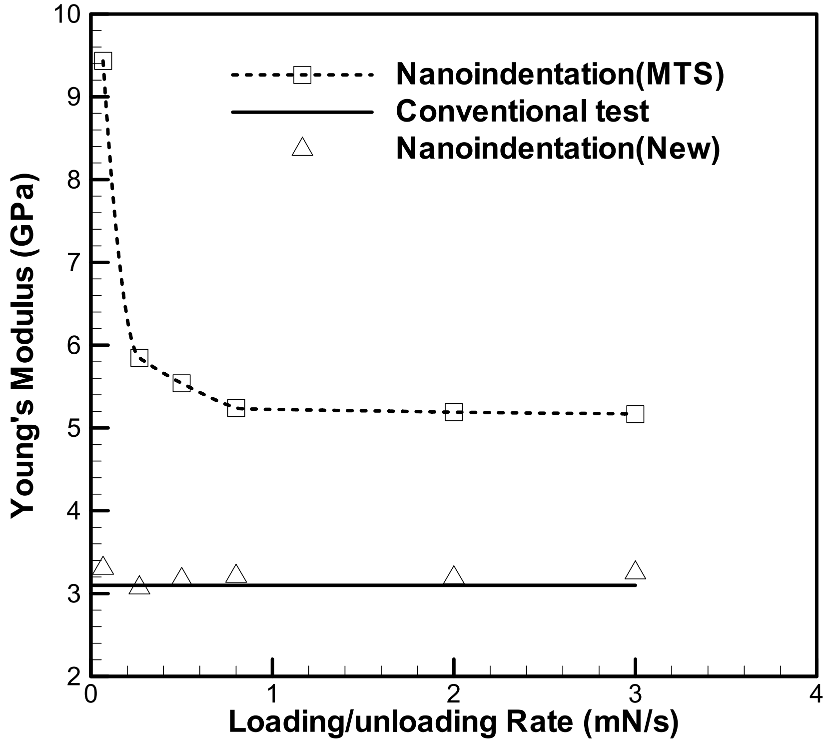

Nanoindentation result for E

(Lu, et al., MTDM, 2003)

Two Approaches in Nanoindentation to Measure the Creep Compliance

Constant Rate loading:

$$P(t) = v_0 t H(t)$$

- Method I:

$$J(t) = \frac{8h}{\pi(1-\nu)\tan\alpha}\frac{dh}{dP}$$

- Method II :

$$h^2(t) = \frac{1}{4}\pi(1-\nu)v_0 \tan\alpha[(J_0 + \sum_{i=1}^{n} J_i)t - \sum_{i=1}^{n} J_i\tau_i(1-e^{-\frac{t}{\tau_i}})]$$

$$J(t) = J_0 + \sum_{i=1}^{n} J_i(1-e^{-t/\tau_i})$$

Step Loading:

$$P(t) = P_0 H(t)$$

$$J(t) = \frac{4h^2(t)}{\pi(1-\nu)P_0\tan\alpha}$$

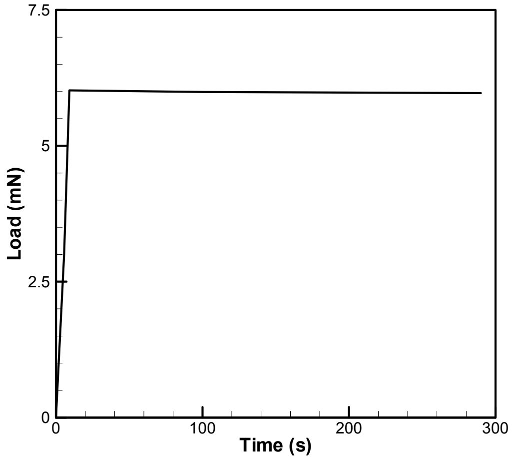

Step Loading
(Ramp Loading in Reality)

(Berkovich indenter, Poisson's ratio is assumed a constant)

Viscoelastic Properties of Foam Parent Material

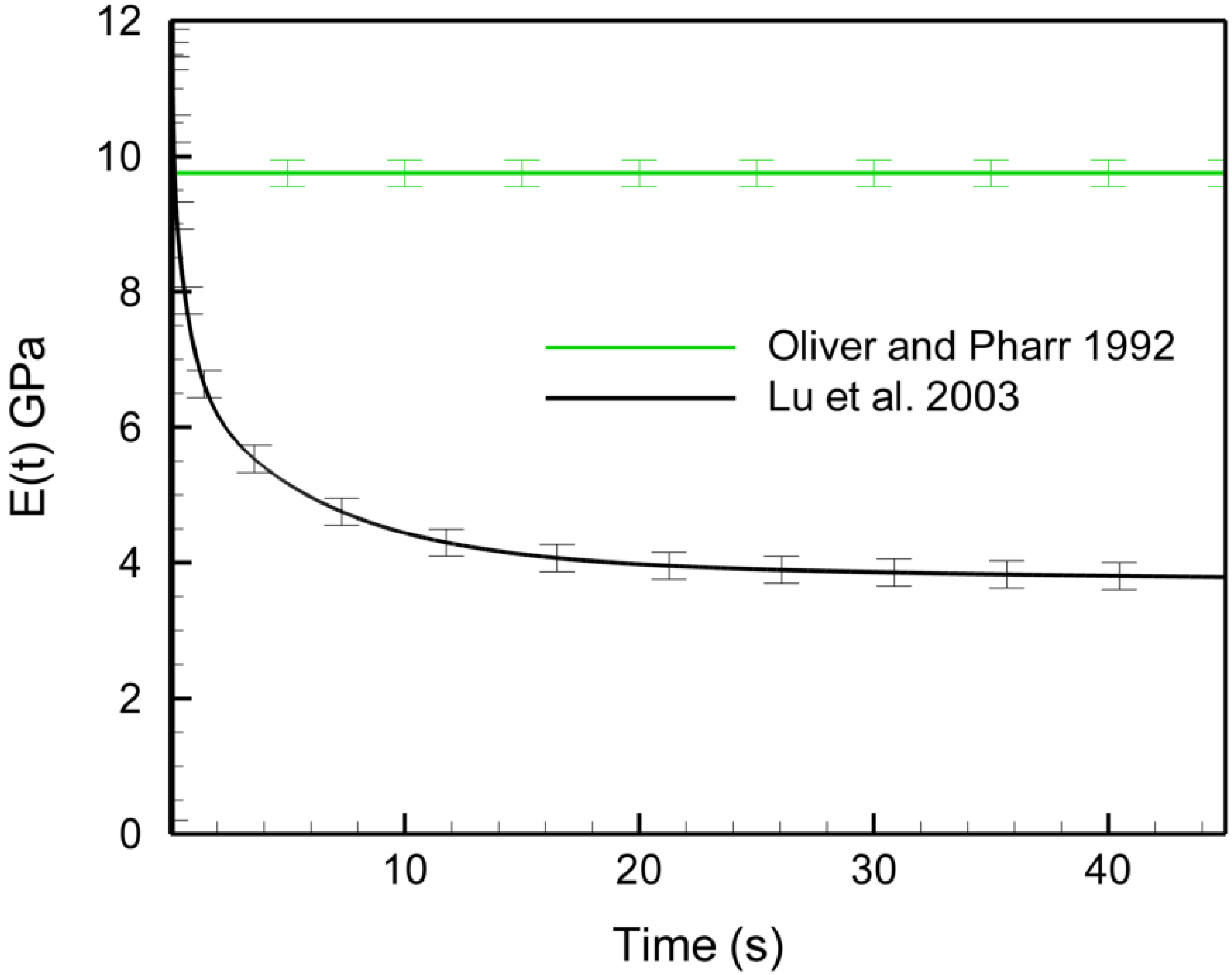

Young’s Relaxation modulus, E_∞ = 3.73 ± 0.2 GPa

Modeling of PMI Foam under Compression

<u>Constitutive model for parent material</u>:
von Mises elastic-plasticity with isotropic bilinear hardening
Density: 1.2 g/cc, Poisson’s ratio: 0.35

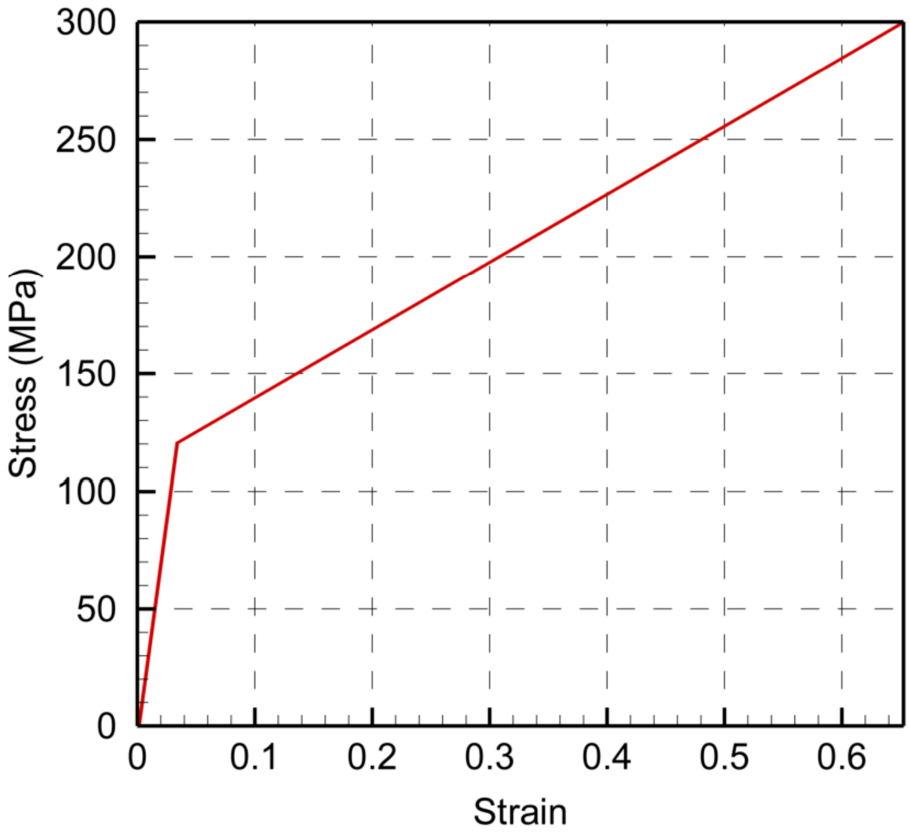

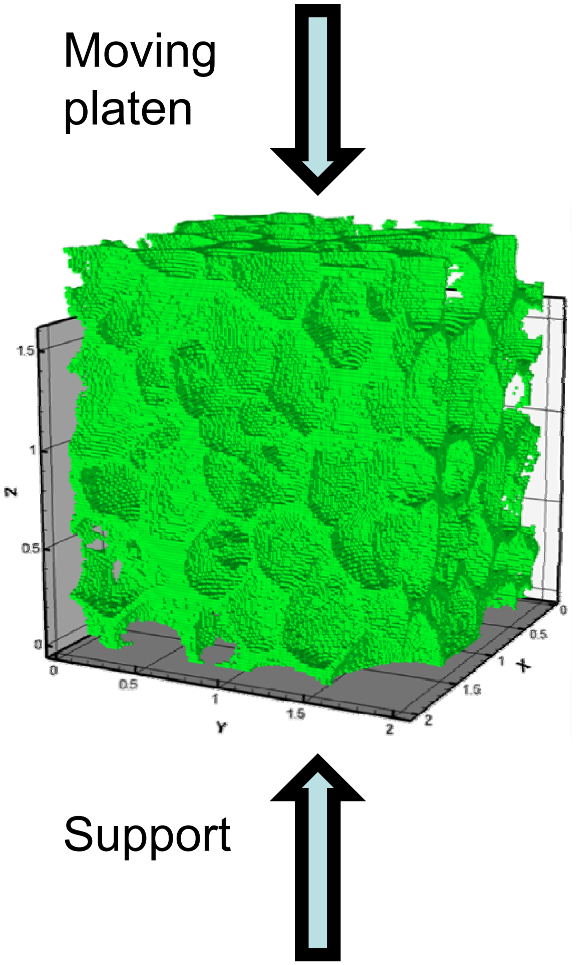

Cell size = 2 × (voxel size)
Cube length = 7x
(where x = 0.3 mm is the unit cell size)

Dynamic Stress Equilibrium Condition

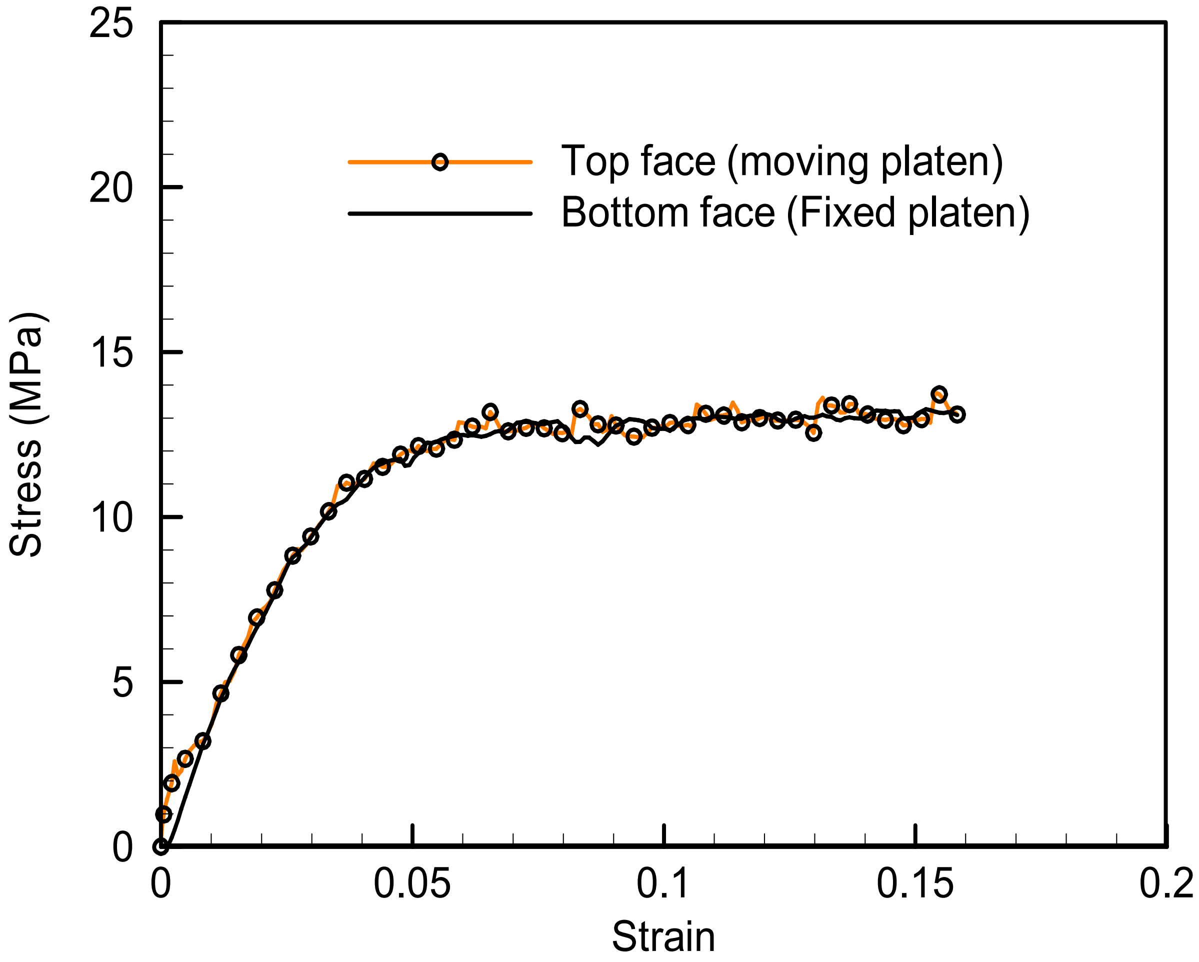

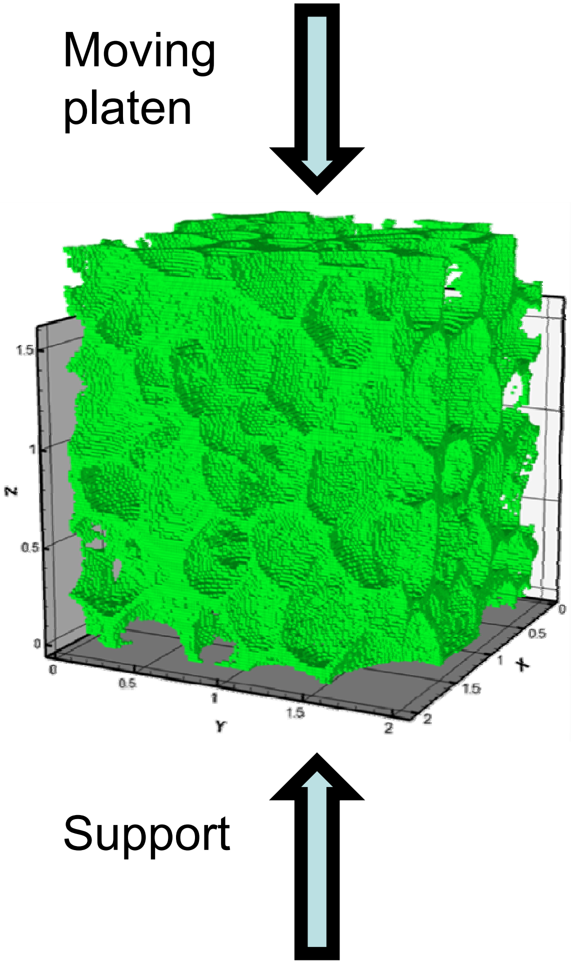

Moving platen

Support

Stress-Strain Curve from GIMP Simulation

Cell-Wall Elastic Properties: E = 3.7 GPa, v = 0.35

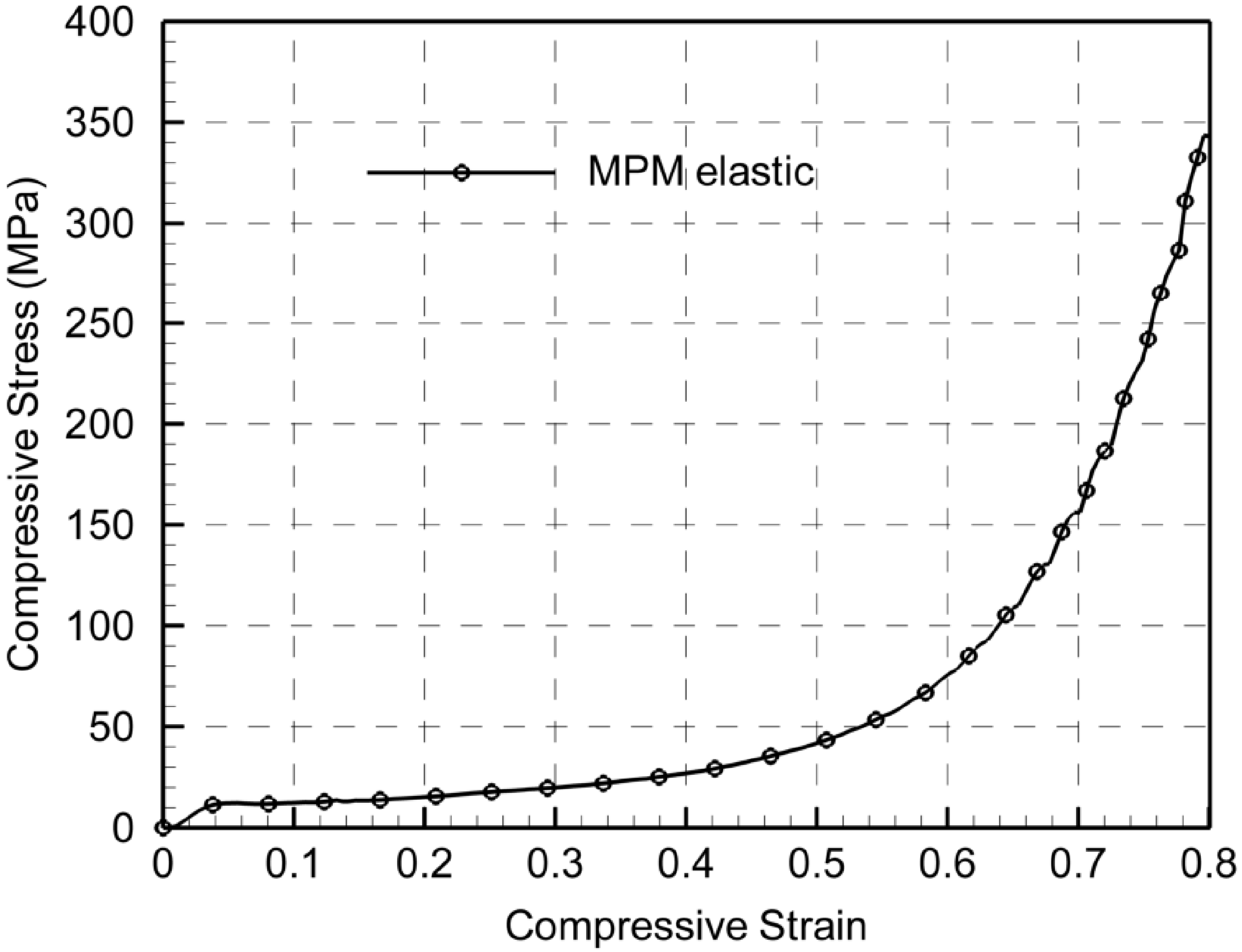

Foam Elastic Properties: E^*_{exp} = 247 MPa, E^*_{MPM} = 303 MPa

Simulation of the Compaction Process (Bi-linear Model)

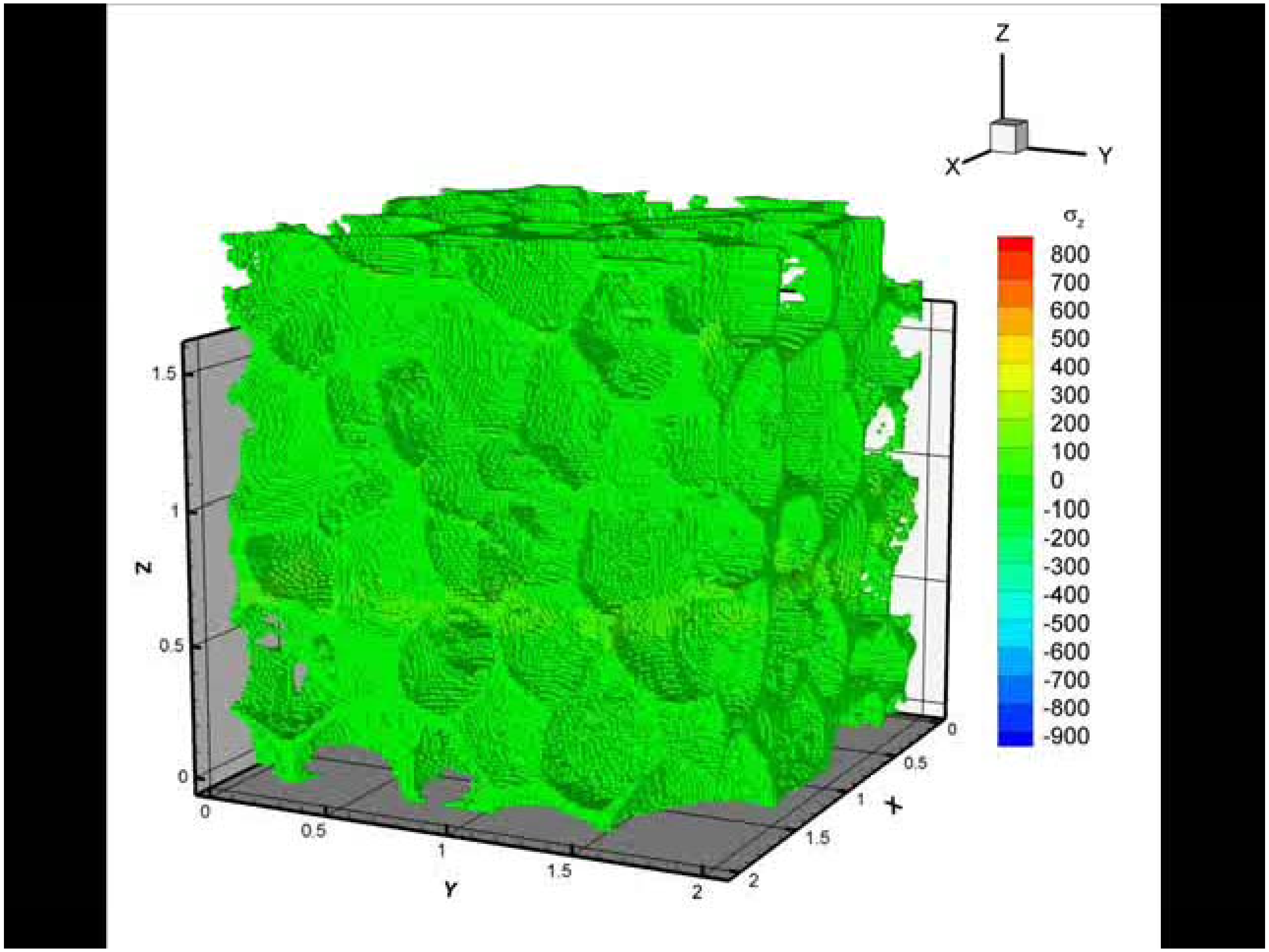

Simulation of the Compaction Process

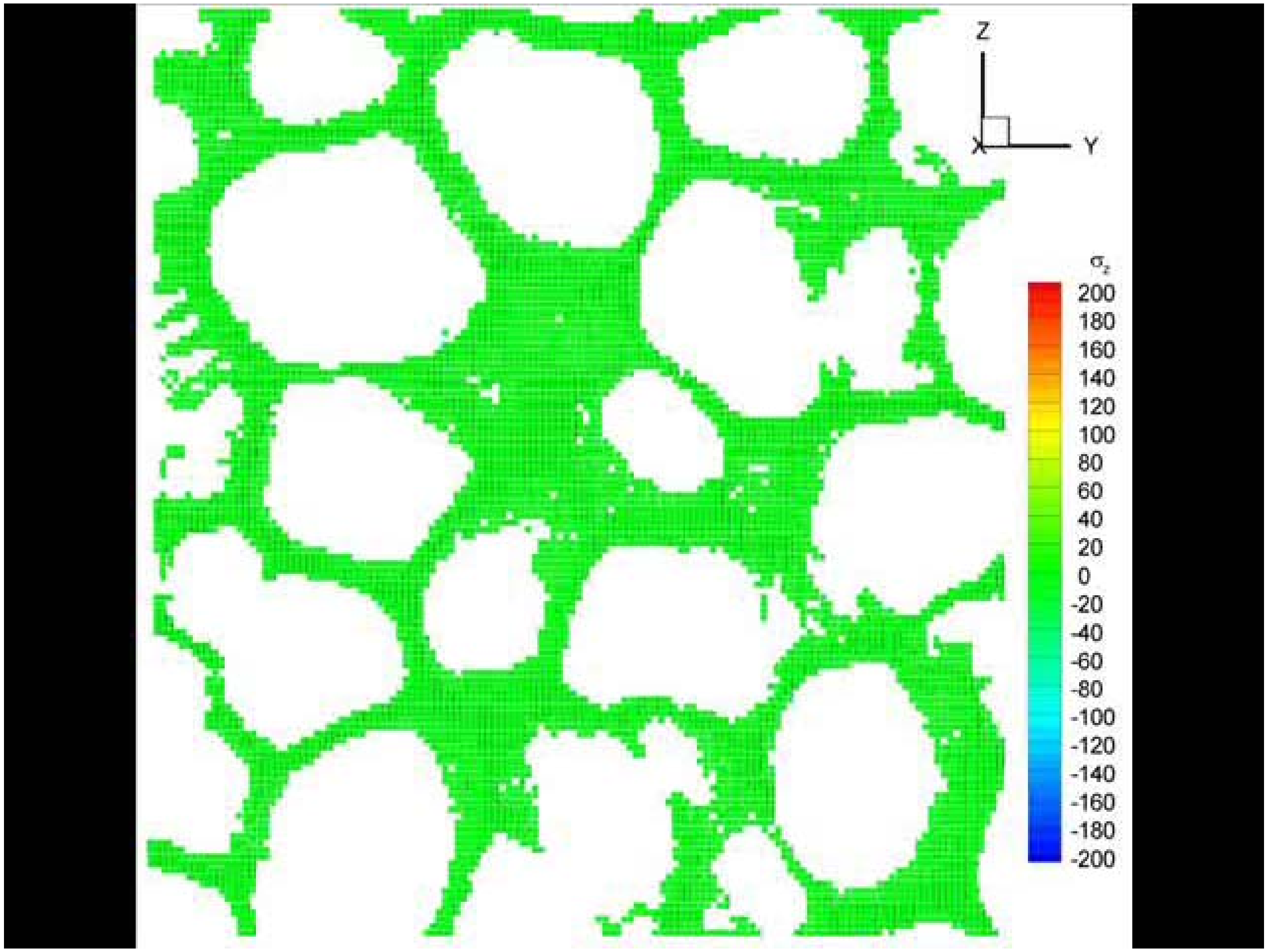

Central section showing stress σ_{zz} (MPa)

Stress-Strain Curve from GIMP Simulation

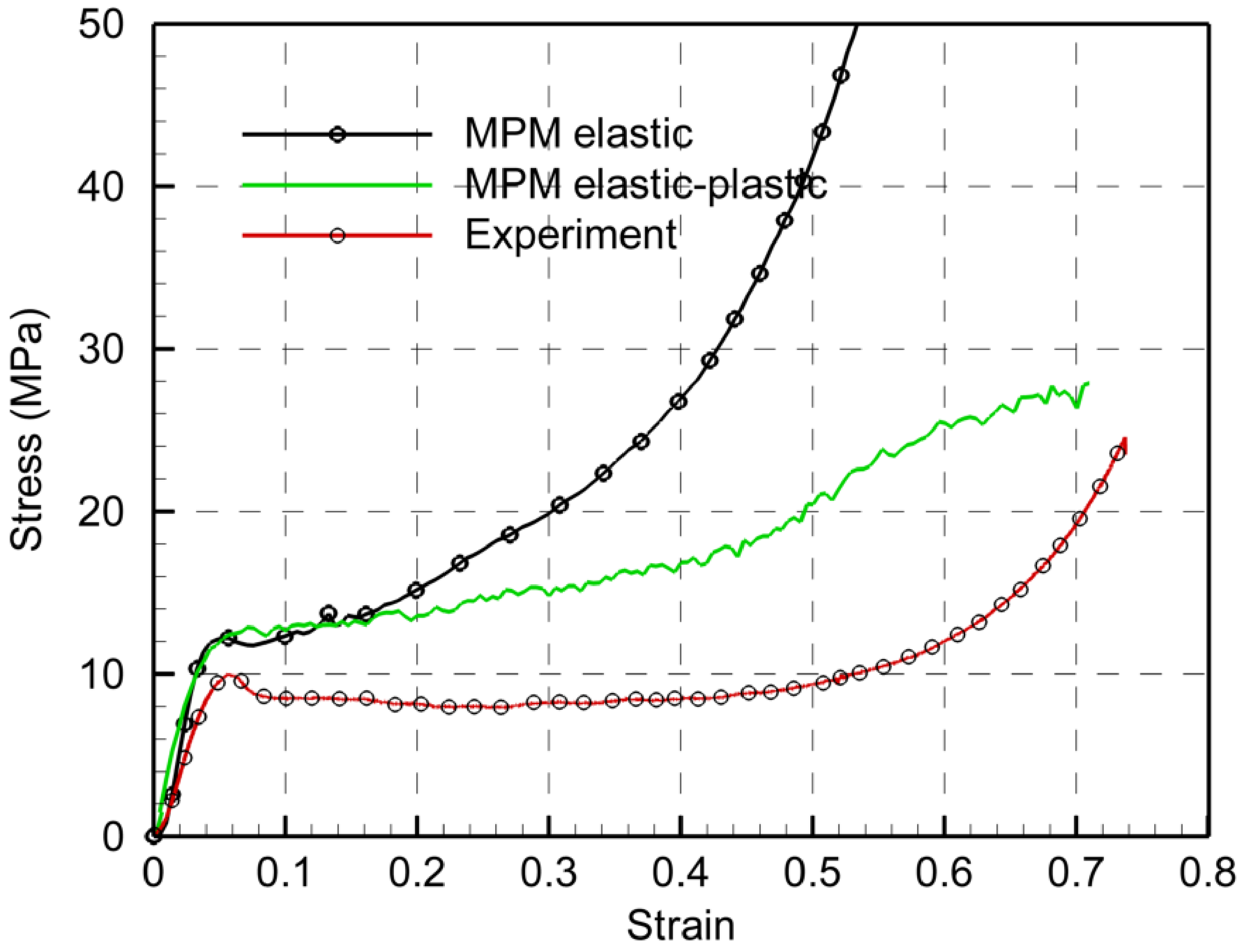

Elastic-plastic properties for cell-walls

Failure stress = 300 MPa

Hardening = 290 MPa

E = 3.7 Gpa

σ_{yield} = 120 MPa

Qualitative Comparison of deformation pattern from simulation with experiment using *in-situ* μ-CT

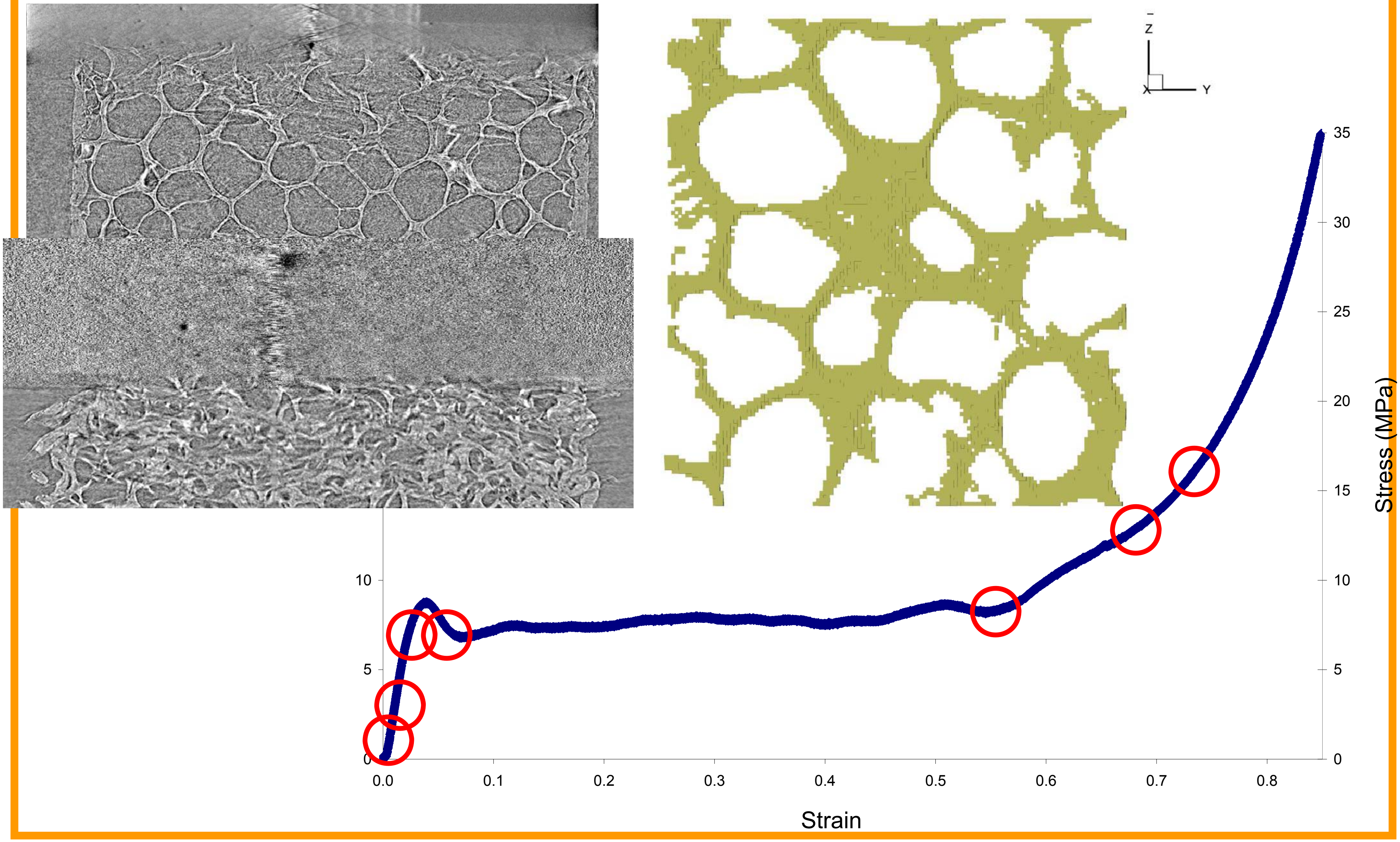

What’s Next?

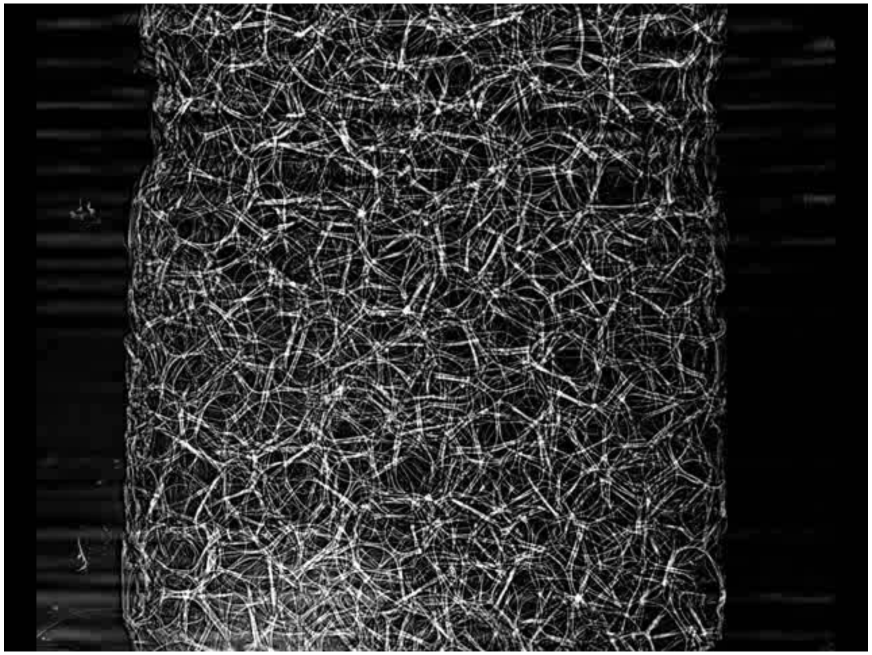

↑ Unconfined compression
Quality not high enough for MPM model generation.

Confined compression →
Preliminary analysis shows that image quality is high.

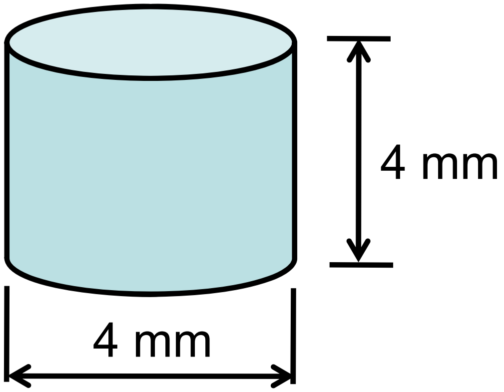

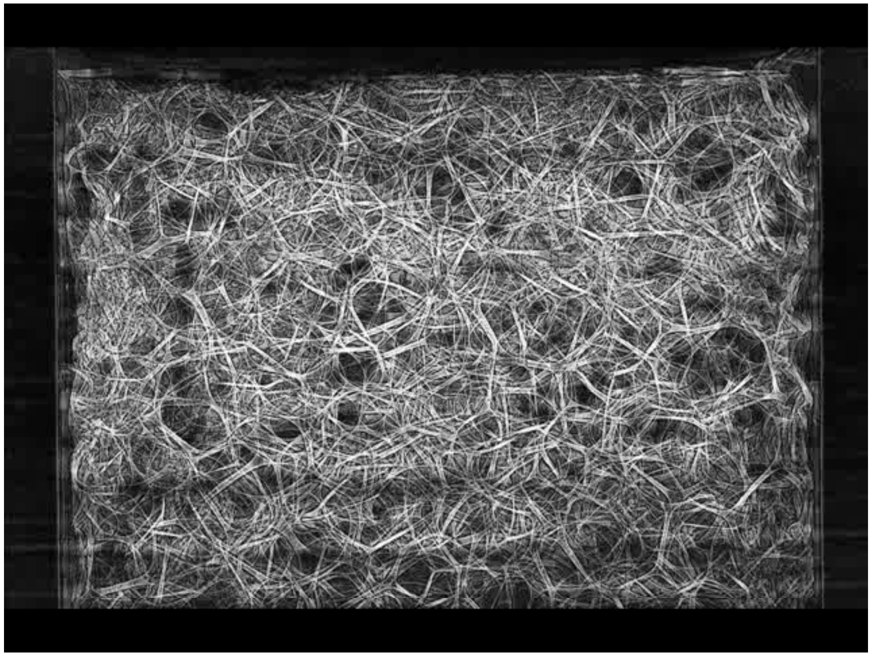

Field of view has 2.8 mm height, a portion of the sample

Other Considerations

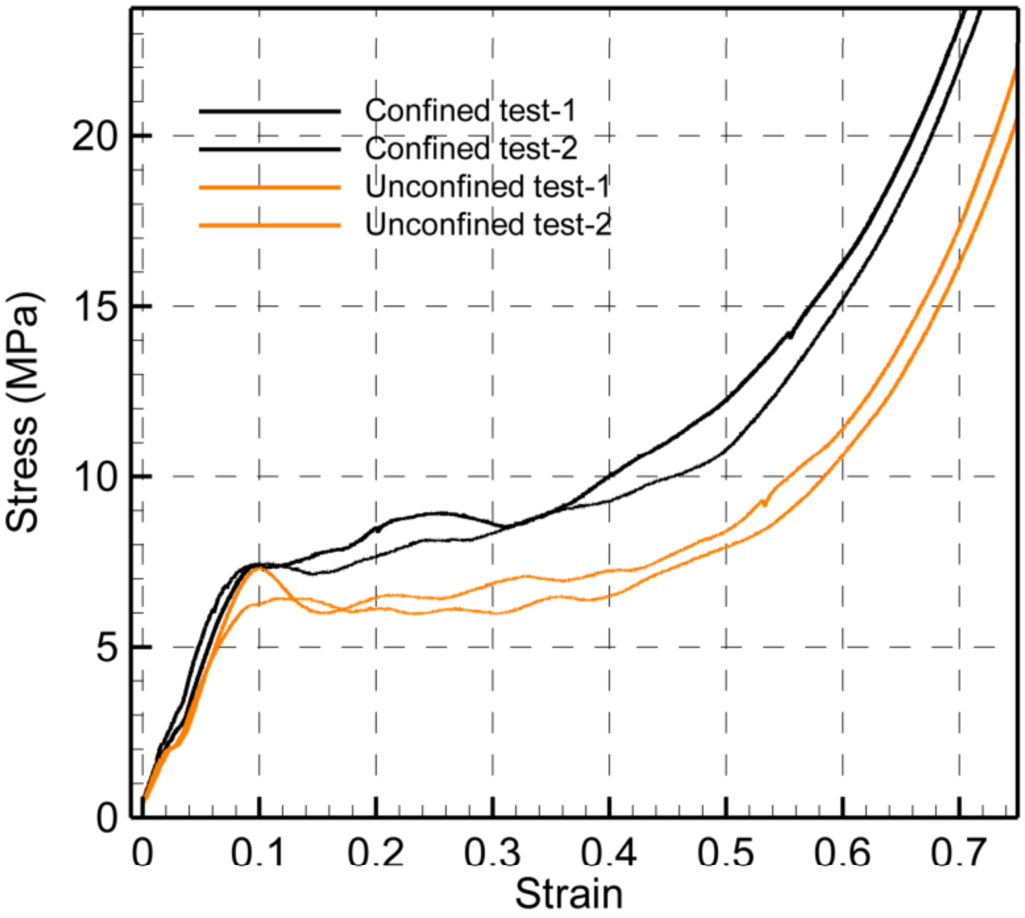

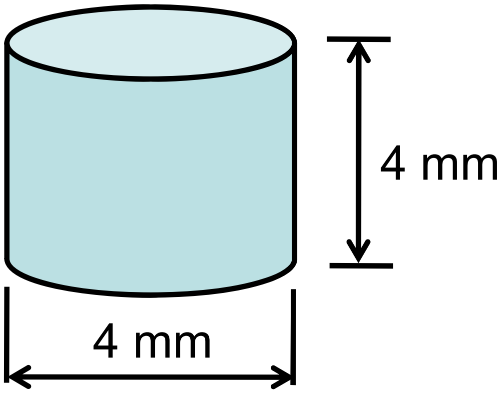

RVE is appropriate for homogeneous Behavior, such as elastic modulus.

For failure analysis, such as compaction, RVE is not necessarily representative. We will simulate the entire sample to investigate the failure behavior.

Issues that need to be addressed:
The complete stress-strain curve;
Nonlinear viscoelasticity;
Contact algorithm; Interpolation induced cell-wall thickening; etc.

Concluding Remarks

- *In-situ* μ-CT tomographic images were acquired during the compression of PMI foam at different strain levels. Tomographic image acquired from Scanco μCT-40 tomography was used to generate MPM model in simulation.

- Viscoelastic nanoindentation was used to determine the steady-state modulus of the cell-walls. The foam elastic modulus was determined with reasonably good agreement. The collapse stress is determined by the elastic buckling of the cell walls, independent of the plastic behavior for the few situations considered.

- The simulated deformed states can capture features in in-situ tomographic images.

- In an attempt to solve an inverse problem, the yield stress and hardening modulus were adjusted in a bi-linear constitutive model, with an attempt to allow the simulated stress-strain curve to have an agreement with experimental data. The drawback of the inverse-problem solving approach is the computational cost.

- Future work is planned to simulate the entire sample under compression, using nonlinear constitutive law determined from nanoindentation measurements.